ESC European Society of Cardiology
Cardiovascular Research
doi:10.1093/cvr/cvy036

Loss of *Sirt3* accelerates arterial thrombosis by increasing formation of neutrophil extracellular traps and plasma tissue factor activity

Daniel S. Gaul[1], Julien Weber[1], Lambertus J. van Tits[1], Susanna Sluka[1], Lisa Pasterk[1], Martin F. Reiner[1], Natacha Calatayud[1], Christine Lohmann[1], Roland Klingenberg[2], Jürgen Pahla[1], Daria Vdovenko[1], Felix C. Tanner[2], Giovanni G. Camici[1], Urs Eriksson[1], Johan Auwerx[3], François Mach[4], Stephan Windecker[5], Nicolas Rodondi[6,7], Thomas F. Lüscher[1,2], Stephan Winnik[1,2†], and Christian M. Matter[1,2*†]

[1]Center for Molecular Cardiology, University of Zurich, Wagistrasse 12, 8952 Schlieren, Switzerland; [2]Department of Cardiology, University Heart Center, University Hospital Zurich, Raemistrasse 100, 8091 Zurich, Switzerland; [3]Laboratory of Integrative and Systems Physiology, Ecole Polytechnique Fédérale de Lausanne, Switzerland; [4]Cardiology Division, Geneva University Hospitals, Switzerland; [5]Department of Cardiology, Swiss Cardiovascular Center Bern, University of Bern, Inselspital Bern, Switzerland; [6]Department of General Internal Medicine, University Hospital Bern; and [7]Institute of Primary Health Care (BIHAM), University of Bern, Switzerland

Received 29 December 2017; revised 29 January 2018; editorial decision 2 February 2018; accepted 9 February 2018

Time for primary review: 24 days

Aims Sirtuin 3 (Sirt3) is a mitochondrial, nicotinamide adenine dinucleotide (NAD^+)-dependent deacetylase that reduces oxidative stress by activation of superoxide dismutase 2 (SOD2). Oxidative stress enhances arterial thrombosis. This study investigated the effects of genetic *Sirt3* deletion on arterial thrombosis in mice in an inflammatory setting and assessed the clinical relevance of these findings in patients with ST-elevation myocardial infarction (STEMI).

Methods and results Using a laser-induced carotid thrombosis model with lipopolysaccharide (LPS) challenge, *in vivo* time to thrombotic occlusion in $Sirt3^{-/-}$ mice ($n = 6$) was reduced by half compared to $Sirt3^{+/+}$ wild-type ($n = 8$, $P < 0.01$) controls. *Ex vivo* analyses of whole blood using rotational thromboelastometry revealed accelerated clot formation and increased clot stability in $Sirt3^{-/-}$ compared to wild-type blood. rotational thromboelastometry of cell-depleted plasma showed accelerated clotting initiation in $Sirt3^{-/-}$ mice, whereas overall clot formation and firmness remained unaffected. *Ex vivo* LPS-induced neutrophil extracellular trap formation was increased in $Sirt3^{-/-}$ bone marrow-derived neutrophils. Plasma tissue factor (TF) levels and activity were elevated in $Sirt3^{-/-}$ mice, whereas plasma levels of other coagulation factors and TF expression in arterial walls remained unchanged. SOD2 expression in bone marrow -derived $Sirt3^{-/-}$ neutrophils was reduced. In STEMI patients, transcriptional levels of Sirt3 and its target SOD2 were lower in $CD14^+$ leukocytes compared with healthy donors ($n = 10$ each, $P < 0.01$).

Conclusions *Sirt3* loss-of-function enhances experimental thrombosis *in vivo* via an increase of neutrophil extracellular traps and elevation of TF suggesting thrombo-protective effects of endogenous Sirt3. Acute coronary thrombosis in STEMI patients is associated with lower expression levels of *SIRT3* and *SOD2* in $CD14^+$ leukocytes. Therefore, enhancing *SIRT3* activity by pan-sirtuin activating NAD^+-boosters may provide a novel therapeutic target to prevent or treat thrombotic arterial occlusion in myocardial infarction or stroke.

Keywords Sirt3 • Neutrophil extracellular traps • Tissue factor • Arterial thrombosis

* Corresponding author. Tel: +41 44 635 6467; fax: +41 44 635 6827, E-mail: christian.matter@uzh.ch; Tel: +41 44 255 3871; fax: +41 44 255 4251, E-mail: christian.matter@usz.ch
† The last two authors contributed equally to the study.

1. Introduction

Myocardial infarction is caused by acute thrombotic occlusion of an epicardial coronary artery and accounts for almost 20% of deaths in Europe in 2015.[1] A major trigger of arterial thrombosis is endothelial activation or dysfunction, which activates tissue factor (TF), a key initiator of the coagulation cascade. In the context of an acute myocardial infarction, the formation of coagulation factors is enhanced by inflammatory stimuli and reactive oxygen species (ROS) thereby accelerating thrombus formation by increasing platelet activation and aggregation and by inhibiting fibrinolysis.[2] Furthermore, activated endothelial cells express adhesion molecules that recruit platelets, monocytes, and neutrophils. Interestingly, neutrophils are among the first cells to reach sites of endothelial activation and damage, where they bind to expressed adhesion molecules or exposed subendothelial layers stimulate the expression of TF and thereby initiate coagulation. In line with this concept, inhibiting neutrophil adhesion is associated with reduced amounts of TF.[3]

Neutrophils exhibit several lines of defence for pathogen elimination in the blood stream, i.e. degranulation, phagocytosis, and formation of neutrophil extracellular traps (NETs), an event where ROS play a key role.[4] NET formation has been considered a programmed cell death mechanism (Enosis), whereby the intracellular content of neutrophils is externalized in a web-like structure that is able to kill microbes.[5] This view has recently been challenged by observations that NETs mainly consist of *mitochondrial* DNA and that neutrophils remain viable after releasing NETs. A trigger of NET formation is bacterial endotoxemia, which is derived from the gut microbiome and induces a pro-inflammatory state that is associated with cardiovascular disease (CVD) in humans.[6] One of the endotoxins that accelerate CVD is lipopolysaccharide (LPS), a component of the bacterial cell membrane. In neutrophils, LPS induces ROS production and enhances NET formation.[5,7] NETs display strong prothrombotic properties as they bind several proteins such as TF that initiate coagulation and promote thrombin generation.[8,9] Indeed, NETs have been associated with the severity of atherosclerosis and thrombosis and have been identified in human coronary thrombi, at lesion sites of ST-elevation myocardial infarction (STEMI).[10]

Sirtuins comprise a family of seven highly conserved nicotinamide adenine dinucleotide (NAD^+)-dependent deacetylases and ribosylases with protective effects in aging, apoptosis, inflammation, and oxidative stress.[11,12] Evidence for a putative role of sirtuins in thrombosis is limited to a study of pharmacological *inhibition* of the nuclear sirtuin 1 (*Sirt1*), which augments arterial thrombosis by increasing TF expression and activity through activation of NFκB,[13] and an associative study suggesting that inhibition of sirtuin 1, 2 or 3 worsens thrombosis by inducing apoptosis-like changes in platelets.[14]

Mitochondrial sirtuin 3 (Sirt3) maintains mitochondrial function in low-energy conditions and activates anti-oxidant defence mechanisms.[15] Sirt3 deacetylases and thus, activates superoxide dismutase 2 (Sod2), the main scavenger of superoxide radicals in mitochondria.[16] Sirt3 also upregulates expression of Sod2 and catalase, another ROS scavenger in the mitochondria.[17] Along these lines, a protective role of Sirt3 has been implicated in metabolic, age-, and oxidative stress-related diseases.[18] Interestingly, *Sirt3*$^{-/-}$ mice exhibit mitochondrial protein hyperacetylation, but remain metabolically normal under basal conditions. Indeed, histological examinations of liver, brown adipose tissue, heart, brain, kidney, and skeletal muscle, mitochondrial numbers, body weight, and fat content, as well as energy balance were not different when comparing *Sirt3*$^{-/-}$ mice to their wild-type (WT) littermates.[19] However, loss of *Sirt3* in combination with a high-cholesterol diet is sufficient to disturb this equilibrium: Under these conditions, the metabolic derangement increases oxidative stress in endothelial mitochondria and induces mild endothelial dysfunction.[20] Notably, the role of *Sirt3* in arterial thrombosis remains unknown. Thus, we hypothesized that constitutive *Sirt3* loss-of-function increases oxidative stress in vascular cells, increases procoagulant properties and eventually accelerates arterial thrombus formation.

2. Methods

Primer sequences are available in the supplementary material at *Cardiovascular Research* online.

2.1 Mice

Mice with a germline *Sirt3* deletion were obtained and congenic C57BL6/J *Sirt3*$^{-/-}$ mice were generated through nine generations of backcrosses with C57BL6/J mice.[21,22] *Sirt3*$^{+/+}$ WT and *Sirt3*$^{-/-}$ mice were kept in a temperature-controlled facility with a 12-h light/dark cycle and free access to normal chow and water for 16 weeks. All animal experiments were approved by, and carried out in accordance with local veterinary authorities (Veterinary Office of the Canton Zurich, permit numbers: 239/2013 and ZH023/17), as well as the guidelines from Directive 2010/63/EU and institutional guidelines. Mice were administered an intraperitoneal injection of 5 mg/kg LPS (E. coli O111: B4, Sigma–Aldrich) 10 h prior to experiments or organ harvesting, respectively.

2.2 Laser-induced carotid thrombosis *in vivo*

Carotid thrombosis was performed using male WT and *Sirt3*$^{-/-}$ mice. Mice were anaesthetized using 87 mg/kg sodium pentobarbital (Butler). Rose bengal (Fisher Scientific) was injected in the tail vein at a concentration of 63 mg/kg. The right common carotid artery was exposed following a midline cervical incision. A Doppler flow probe (Transonic Systems) was applied and connected to a flowmeter (Transonic, Model T106) and a 1.5mW green laser (540 nm; Melles Griot) was applied to the site of injury at a distance of 6 cm for 60 min. Blood flow was monitored from laser onset for maximum 120 min, or until occlusion (flow ≤0.1 mL for 1 min) occurred.

2.3 NET formation

Neutrophils were isolated from mouse bone marrows (BM) using gradient centrifugation.[23] For each condition, 50 000 cells were plated into one well of a black, clear-bottom 96 well plate (Corning) and incubated for 30 min at 37°C. All wells were then supplied with 5 µM SYTOX Green (ThermoFisher Scientific) and, thereafter, stimulated with 2 µg/mL LPS (E. coli O111: B4, Sigma–Aldrich) or vehicle control. Fluorescence (ex/em = 488/523) was measured every 5 min over 4 h at 37°C in a plate reader (Tecan).

2.4 Human samples

Patients with acute coronary syndromes (ACS) were prospectively enrolled between 2009 and 2012 into the multicentre Swiss SPUM-ACS cohort (NCT01000701). Inclusion criteria for this subgroup of patients recruited at the University Hospital Zurich comprised diagnosis of STEMI, age ≥18 years and presentation within 72 h after pain onset. Exclusion criteria were severe physical disability, inability to comprehend study or life expectancy <1 year for non-cardiac reasons.

Healthy individuals were recruited from the local blood bank and invited for an outpatient visit at University Hospital Zurich. Individuals were eligible if none of the following exclusion criteria were found by history, clinical exam, blood analysis or echocardiogram: Age <18 years, use of cardiovascular medication, positive cardiovascular family history, smoking (including cessation of smoking within 2 years prior to study enrolment), history of hypertension, elevated total cholesterol (≥5.0 mmol/L), BMI > 30 kg/m^2, history of diabetes mellitus, evidence of relevant valvular or structural heart disease and/or a reduced LV ejection fraction (LVEF; <55%) on echocardiogram.

In STEMI patients, blood was drawn at the beginning of catheterization (after sheath insertion). Leukocytes were separated from whole blood by Ficoll density gradient centrifugation (400× RCF, 30 min at 22°C). Cells were stained for 10 min on ice using human CD14-FITC antibody (Miltenyi Biotec) and subsequently sorted using a FACSAria III 4 L (BD Biosciences). RNA of CD14$^+$ cells was isolated and analysed as described in the Supplemental material online.

The study complies with the Declaration of Helsinki, and the locally appointed ethics committee approved the research protocol. Informed consent was obtained from all subjects.

2.5 Rotational thromboelastometry

Whole blood was taken from the mice by right ventricular puncture and decalcified by adding 1/10 (v/v) 3.2% sodium citrate. For plasma analyses, decalcified whole blood was centrifuged for 10 min at 2000×*g* and the resulting plasma supernatant was used. Whole blood was analysed in the rotational thromboelastometry (ROTEM) delta machine according to the manufacturer's instructions using the star-tem, fib-tem, and ex-tem reagents. Plasma was analysed using the ROTEM mini accessories to allow for smaller volumes (equipment and reagents by Tem International GmbH).

2.6 ELISA

Plasma was derived from whole blood as described earlier and was subjected to ELISA for quantifying levels of coagulation factors V, VII, and IX (all ELISAs from Cloud-Clone Corp.), tissue factor (R&D Systems Inc.) and tissue factor activity according to manufacturer's instructions (Sekisui Diagnostics LLC).

2.7 Whole blood platelet aggregometry

Whole blood was collected as described earlier. Whole blood was diluted 1:3 in 0.9% saline and aggregometry performed in response to thrombin (2 U/mL, Sigma–Aldrich) at 37°C using impedance aggregometry (Chrono-log Corporation).

2.8 Expression analyses

Liver and aortae samples were homogenized using the Precellys 24 homogenizer (Bertin technologies). Total RNA was isolated from homogenized samples and from isolated human CD14$^+$ cells using TRI Reagent (Sigma–Aldrich) according to the manufacturer's instructions and mRNA was translated to cDNA using Ready-To-Go You-Prime First-Strand Beads (GE Healthcare). SYBR® green based real-time quantitative PCR (RT-PCR) was carried out according to standard protocol using a Quant Studio 7 Flex Real Time PCR thermocycler (Applied Biosystems) and expression calculated using the $\Delta\Delta C_T$ method normalizing values to expression of GAPDH.

2.9 RT-PCR primers

Primers sequences were obtained from the qPrimer Depot database (https://mouseprimerdepot.nci.nih.gov/; Wenwu Cui PhD, Laboratory of Receptor Biology and Gene Expression, National Cancer Institute, National Institutes of Health). Sequences were synthesized by Microsynth, Switzerland.

2.10 Statistics

Metric variables were assessed for distribution using the D'Agostino-Pearson omnibus normality test. For $n < 8$, non-parametric distribution was assumed. Different groups were compared using unpaired Student's *t* tests for normally distributed data, or Mann–Whitney tests for data with non-parametric distribution. *P* values are two-tailed. Significance was accepted for $P < 0.05$. Data are presented as mean ± SD (scatter plots and table) or as mean ± SEM (time-dependent curves). Statistical analyses were performed using Prism 6 for Mac OS X (GraphPad Software).

3. Results

3.1 Loss of *Sirt3* accelerates time to arterial thrombotic occlusion in an inflammatory setting *in vivo*

To assess the effects of *Sirt3* loss-of-function on thrombosis, time to arterial occlusion was analysed in *Sirt3*$^{-/-}$ and *Sirt3*$^{+/+}$ WT mice following laser-induced carotid endothelial injury after lipopolysaccharide (LPS) challenge (*Figure 1A–E*). Compared to WT controls, *Sirt3*$^{-/-}$ mice showed a 55% reduction in time to occlusion (*Figure 1B*). A representative blood flow tracing of one individual animal of each group shows the reduction of blood flow over the time course of the experiment. The line at 0.1 mL/min indicates the threshold flow regarded as carotid occlusion (*Figure 1C*). Initial blood flow and heart rate did not differ between the two groups (*Figure 1D* and *E*).

3.2 Loss of *Sirt3* enhances clot formation and increases clot firmness *ex vivo*

The effects of *Sirt3* deficiency on clotting properties of whole blood were investigated using ROTEM (*Figure 2A*). Tomograms analyses from WT (*Figure 2B*) and *Sirt3*$^{-/-}$ whole blood (*Figure 2C*) revealed that *Sirt3*$^{-/-}$ mice displayed an accelerated clotting time (CT, i.e. time to initiation of clotting) (*Figure 2D*) and decreased clot formation time (CFT, i.e. time between initiation of clotting and a clot strength of 20 mm amplitude) (*Figure 2E*). Clot firmness was increased over the course of the entire experiment in whole blood of *Sirt3*$^{-/-}$ mice compared to WT controls (*Figure 2F*). Area under the curve analyses revealed a 30% increase in clot firmness in *Sirt3*$^{-/-}$ mice compared to the control group (*Figure 2G*). The maximum clot firmness was increased in the *Sirt3*-deficient group (*Figure 2H*), whereas time to maximum clot firmness was decreased in *Sirt3*$^{-/-}$ compared to WT controls (*Figure 2I*). These data indicate that *Sirt3*$^{-/-}$ mice exhibit altered blood clotting properties independent of the vessel wall, that cause accelerated thrombotic carotid occlusion *in vivo*.

3.3 Transcription levels of thrombosis-associated genes in mouse aortic lysates do not differ between *Sirt3*$^{-/-}$ and WT mice

To address the involvement of the arterial wall, we assessed transcription of key pro- or anticoagulant genes in mouse aortic lysates. These

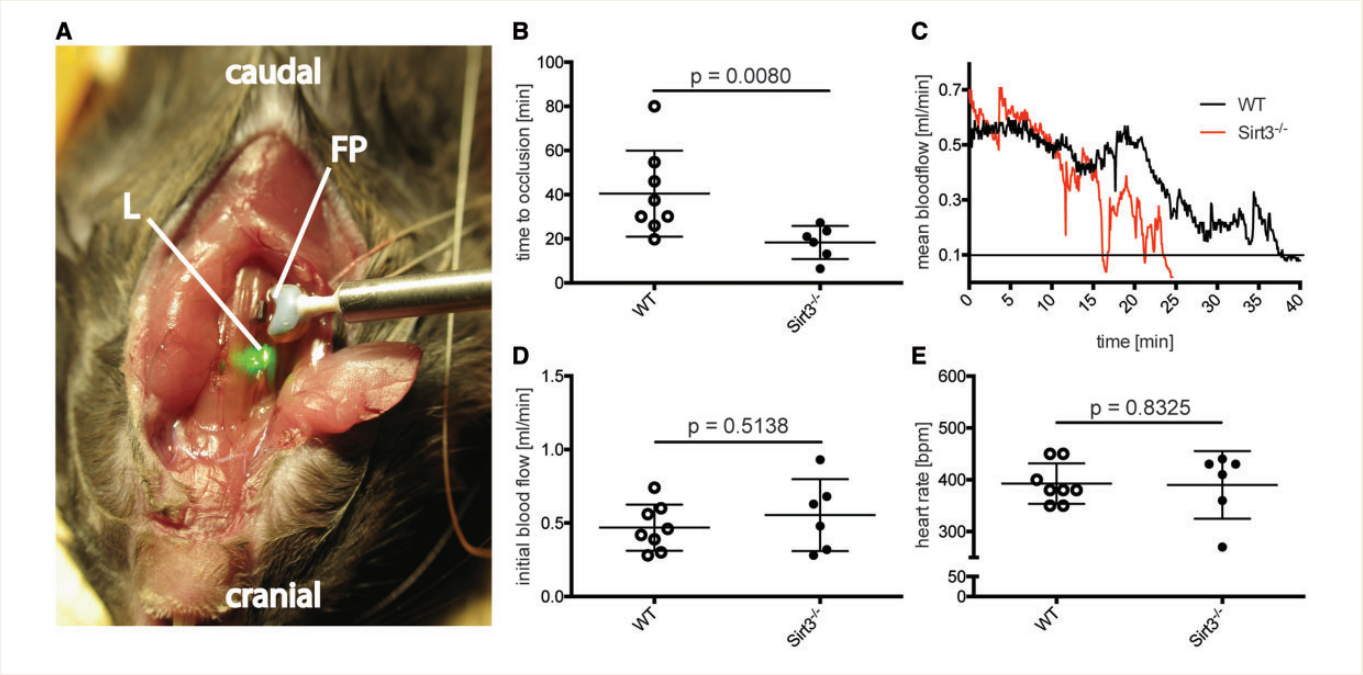

Figure 1 Loss of *Sirt3* accelerates time to carotid thrombotic occlusion *in vivo*. Mouse model of laser-induced carotid thrombosis (*A*): The right carotid artery was dissected and blood flow measured using a Doppler flow probe (FP). A laser (L) pointing at the carotid artery was exciting a previously intravenously injected photo-reactant resulting in endothelial damage and subsequent thrombus formation. Time to thrombotic occlusion in *Sirt3*$^{-/-}$ mice was cut in half compared to WT controls following lipopolysaccharide (LPS) challenge (*B*). The tracing shows mean blood flow until occlusion (mean flow ≤ 0.1 mL for 1 min) (*C*). Initial blood flow and heart rate remained unaltered between the groups (*D* and *E*). $n \geq 6$, Mann–Whitney test was used for statistical analysis of all graphs.

analyses revealed no difference in transcription levels of *Ft*., Tf pathway inhibitor (*Tfpi*), von Willebrand factor (*vWf*), plasminogen activator inhibitor 1 (*Pai-1*), *Pai-2*, thrombomodulin (*Thbd*), intercellular adhesion molecule 1 (*Icam-1*), vascular cell adhesion molecule 1 (*Vcam-1*) or tissue plasminogen activator (*tPa*), respectively (see Supplementary material online, *Figure S1A–I*).

3.4 Cell and platelet depletion in *Sirt3*$^{-/-}$ blood normalize clot formation time and clot firmness

To differentiate between the contribution of corpuscular vs. soluble blood components, ROTEM experiments were repeated using platelet-poor plasma (*Figure 3A*). The TEMogram of WT plasma (*Figure 3B*) vs. *Sirt3*$^{-/-}$ plasma (*Figure 3C*) revealed that the clotting time was decreased in *Sirt3*-deficient plasma (*Figure 3D*). Of note, the differences in clot formation time and clot firmness observed in ROTEM experiments using whole blood were abolished in the absence of blood cells and platelets (*Figure 3E–I*), suggesting a role of these blood components in *Sirt3*-mediated thrombosis.

3.5 Platelets do not play a role in *Sirt3*-mediated thrombosis

Platelet counts did not differ between *Sirt3*$^{-/-}$ and WT mice (see Supplementary material online, *Figure S2A*), nor did *ex vivo* platelet aggregation after stimulation of whole blood with thrombin (see Supplementary material online, *Figure S2B and C*). ROTEM analysis showed that the difference in clotting time was abolished between the two groups after adding exogenous TF and inhibiting platelet aggregation (see Supplementary material online, *Figure S2D*), whereas the other differences in clot formation time, clot firmness over time, and maximal clot firmness persisted (see Supplementary material online, *Figure S2E–H*). No difference in time to maximum clot firmness was observed (see Supplementary material online, *Figure S2I*).

3.6 Exogenous TF accelerates clotting initiation in WT whole blood

ROTEM analysis was performed on whole blood to investigate why the difference in clotting time was lost after inhibition of platelets and addition of exogenous TF (as observed in Supplementary material online, *Figure S2D*). Addition of exogenous TF without platelet inhibition abolished the difference in clotting time (see Supplementary material online, *Figure S3A*). In contrast, the differences in clot formation time, clot firmness over time, and maximal clot firmness persisted between the two groups (see Supplementary material online, *Figure S3B–E*). No difference in time to maximum clot firmness was detected (see Supplementary material online, *Figure S3F*).

3.7 Loss of *Sirt3* favours NET formation in mouse neutrophils

After excluding a platelet contribution in *Sirt3*-mediated thrombosis, we focused on neutrophils, as they have been shown to be the first cells

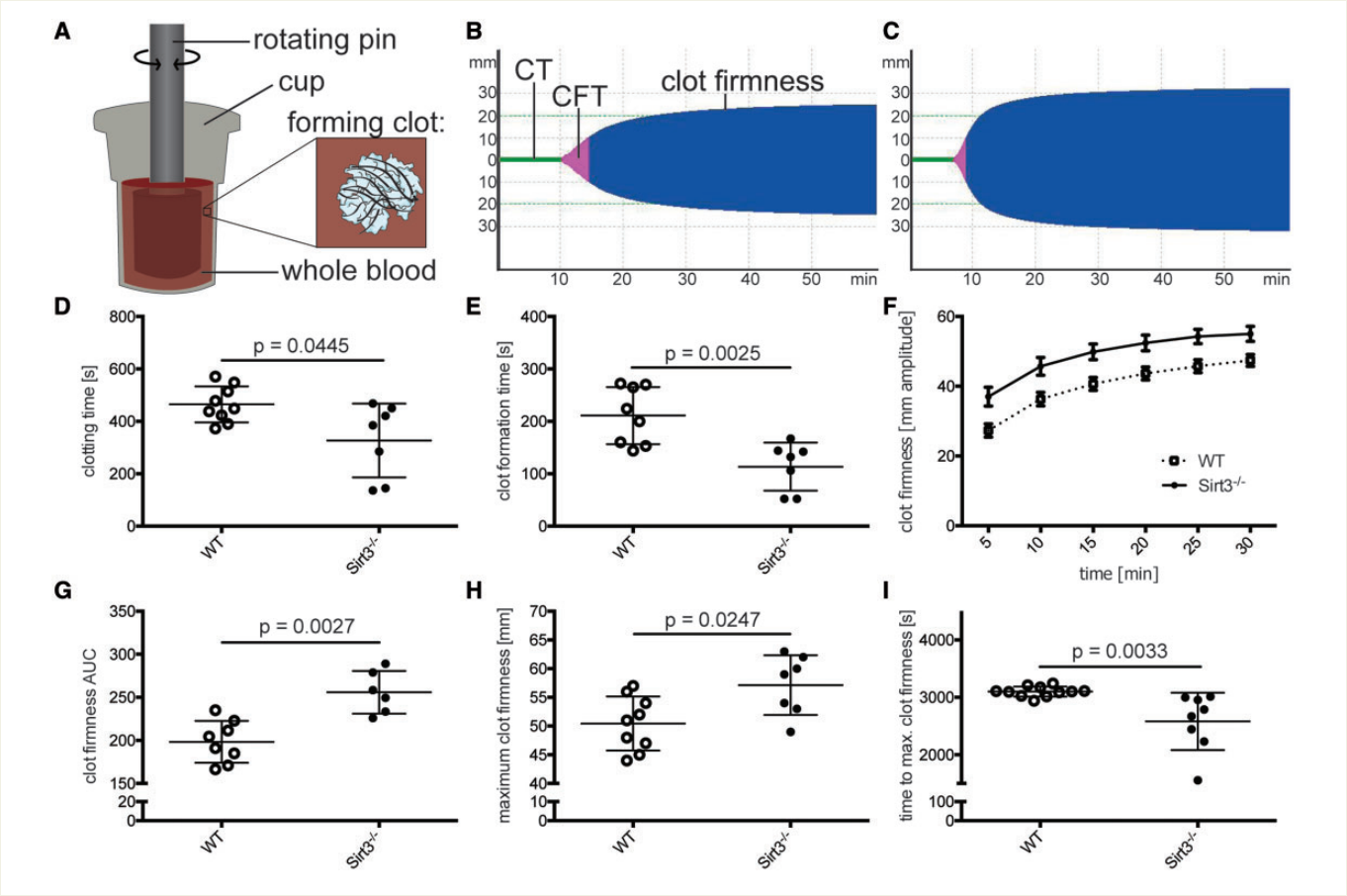

Figure 2 Loss of *Sirt3* accelerates blood clotting and clot firmness *ex vivo*. Whole blood coagulation was assessed using rotational thromboelastometry (ROTEM) (*A*). Once the blood started to coagulate, the rotation of the pin was restricted and the kinetics translated to a TEMogram. Representative pictures show the TEMogram from WT (*B*) compared to *Sirt3*$^{-/-}$ whole blood (*C*). *Sirt3*$^{-/-}$ blood revealed an earlier onset of clotting (*D*) and reached a predefined clot firmness earlier than control mice (*E*). Furthermore, blood of *Sirt3*$^{-/-}$ animals showed increased clot firmness throughout the experiment (*F–H*) and maximum clot firmness was reached earlier (*I*). $n \geq 6$, Student's *t*-test was used in graph (*D*) and (*I*), Mann–Whitney test was applied in graphs (*E*), (*G*), and (*H*). CT, clotting time (time until initiation of clotting); CFT, clot formation time (time between initiation of clotting and a clot strength of 20 mm amplitude).

recruited at the site of endothelial damage. Neutrophils were isolated from BM and stimulated with LPS. NET formation in *Sirt3*$^{-/-}$ compared to WT neutrophils was increased early on after stimulation and persisted for 4 h (*Figure 4A*). Area under the curve analyses revealed a 75% increase in NET formation in *Sirt3*$^{-/-}$ cells over time (*Figure 4B*). Representative photomicrographs of unstimulated WT neutrophils, as well as WT and *Sirt3*$^{-/-}$ neutrophils after 2 h of LPS stimulation show no difference in unstimulated vs. stimulated WT cells and a typical net-like externalization of DNA in the *Sirt3*$^{-/-}$ group (*Figure 4C*). Fluorescence-activated cell sorting (FACS) analysis for the neutrophil markers Ly6G and CD11b identified 83% of isolated cells as neutrophils (*Figure 4D*) and >97% as viable (*Figure 4E*).

3.8 Loss of *Sirt3* increases plasma tissue factor expression and activity

To address the difference in clotting time between *Sirt3*$^{-/-}$ and WT controls observed using ROTEM (*Figure 2D*), and its rescue upon exogenous TF (see Supplementary material online, *Figures S2D and S3A*), plasma was analysed for TF levels and activity. *Sirt3*$^{-/-}$ mice displayed higher levels of soluble TF than WT controls (*Figure 5A*). Increased levels of TF translated into increased TF activity in the plasma of *Sirt3*$^{-/-}$ mice compared to WT controls (*Figure 5B*). As coagulation factors are predominantly synthesized in the liver, liver lysates were analysed. Expression analyses revealed elevated mRNA levels of the coagulation factors V, VII, and IX in *Sirt3*$^{-/-}$ mice (*Figure 5C*). However, these results did not translate into corresponding changes in plasma protein (*Figure 5D*).

3.9 From mice to men—reduced *Sirt3* and *SOD2* levels in CD14^{+} leukocytes of STEMI patients

When comparing BM-derived neutrophils from *Sirt3*$^{-/-}$ and WT mice by real-time quantitative PCR, cells lacking *Sirt3* (*Figure 6A*) showed reduced transcription of *Sod2* (*Figure 6B*). In humans with acute coronary occlusion and STEMI, PCR analyses of CD14^{+} leukocytes exhibited reduced transcription levels of both *SIRT3* (*Figure 6C*) and its downstream target *SOD2* (*Figure 6D*) when compared to the respective cell population of

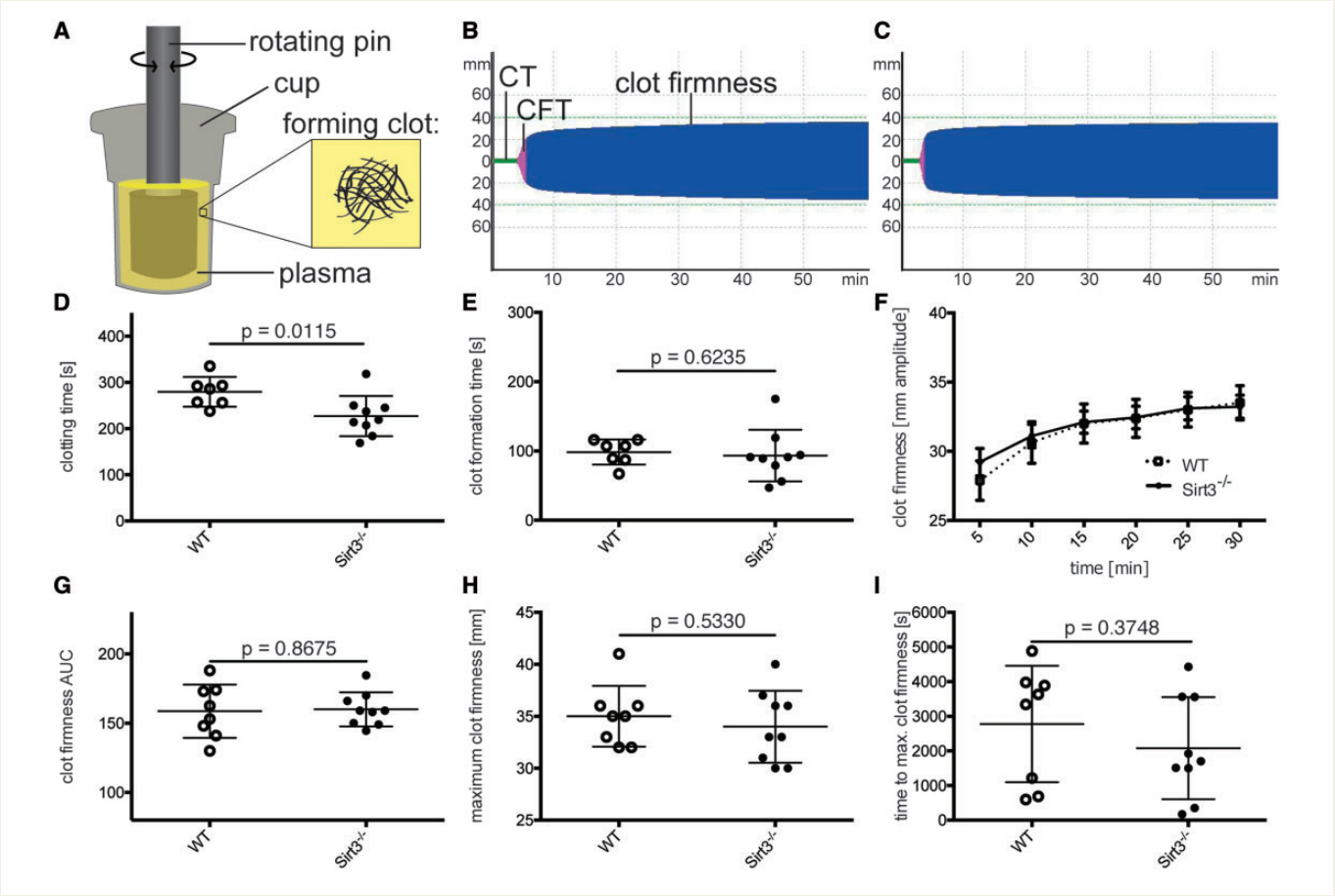

Figure 3 Cell depletion of *Sirt3*$^{-/-}$ blood rescues clot formation time and clot firmness, but not time to initiation of clotting. Murine plasma depleted of all cells was analysed using ROTEM (*A*). Once the factors in the plasma started to coagulate, the rotation of the pin was restricted and the kinetics translated to a TEMogram. Representative pictures show the TEMogram from WT (*B*) compared to *Sirt3*$^{-/-}$ plasma (*C*). Clotting time was reduced in *Sirt3*$^{-/-}$ vs. WT plasma (*D*). No differences could be observed in all other parameters after depleting the blood of cellular components (*E–I*). $n \geq 7$, Student's *t*-test was used to analyse graphs (*D*) and (*E*) and graphs (*G–I*) were analysed with the Mann–Whitney test. CT, clotting time (time until initiation of clotting); CFT. clot formation time (time between initiation of clotting and a clot strength of 20 mm amplitude).

healthy donors. However, mouse CD11b^{+} cells lacking *Sirt3* (*Figure 6D*) showed no difference in *Sod2* transcription compared to corresponding WT cells (*Figure 6E*). Of note, baseline characteristics of STEMI patients and healthy donors did not significantly differ for age, gender, BMI, systolic blood pressure, LDL-cholesterol, and diabetes mellitus—parameters potentially relevant for Sirt3 (*Table 1*). Increased stress-induced levels of glucose, C-reactive protein (CRP), and diastolic blood pressure are to be expected in the acute setting of STEMI as compared to the quiescent context of healthy donors.

4. Discussion

We here show that genetic loss of *Sirt3* in mice accelerates carotid artery occlusion *in vivo* under pro-inflammatory conditions. *Ex vivo* ROTEM revealed accelerated clot initiation, clot formation, and increased clot stability in *Sirt3*-deficient mice. These events were associated with enhanced formation of thrombogenic NETs, increased expression, and activity of TF in plasma and reduced *Sod2* transcription in neutrophils. In CD14^{+} leukocytes isolated from STEMI patients with an acute coronary occlusion, transcription levels of *SIRT3*, and its downstream target *SOD2* were reduced compared to healthy donors.

In the context of thrombosis, formation of NETs is detrimental because of their pro-coagulant properties. NETs bind von Willebrand factor, fibronectin, and fibrinogen, contain inhibitors of the anticoagulant TFPI, provide a large surface for TF and active coagulation factor XII, and promote thrombin generation.[8,9,24] These properties provide a scaffold for the binding of platelets and coagulation factors. They also comprise stimuli for platelet aggregation and activating the coagulation cascade. Eventually, these events accelerate clot formation and enhance clot stability, as observed in our *ex vivo* model.

NET formation can be triggered by ROS and a recent study has demonstrated that mitochondrial ROS are sufficient to generate NETs.[4] *Sirt3* activates transcription of *Sod2*, thereby scavenging mitochondrial ROS. Our findings support the association between mitochondrial ROS and NET formation by showing that loss of *Sirt3* decreases *Sod2* transcription and increases NET formation. The causal role of *Sirt3* in protecting neutrophils from oxidative stress-induced NET formation in animal

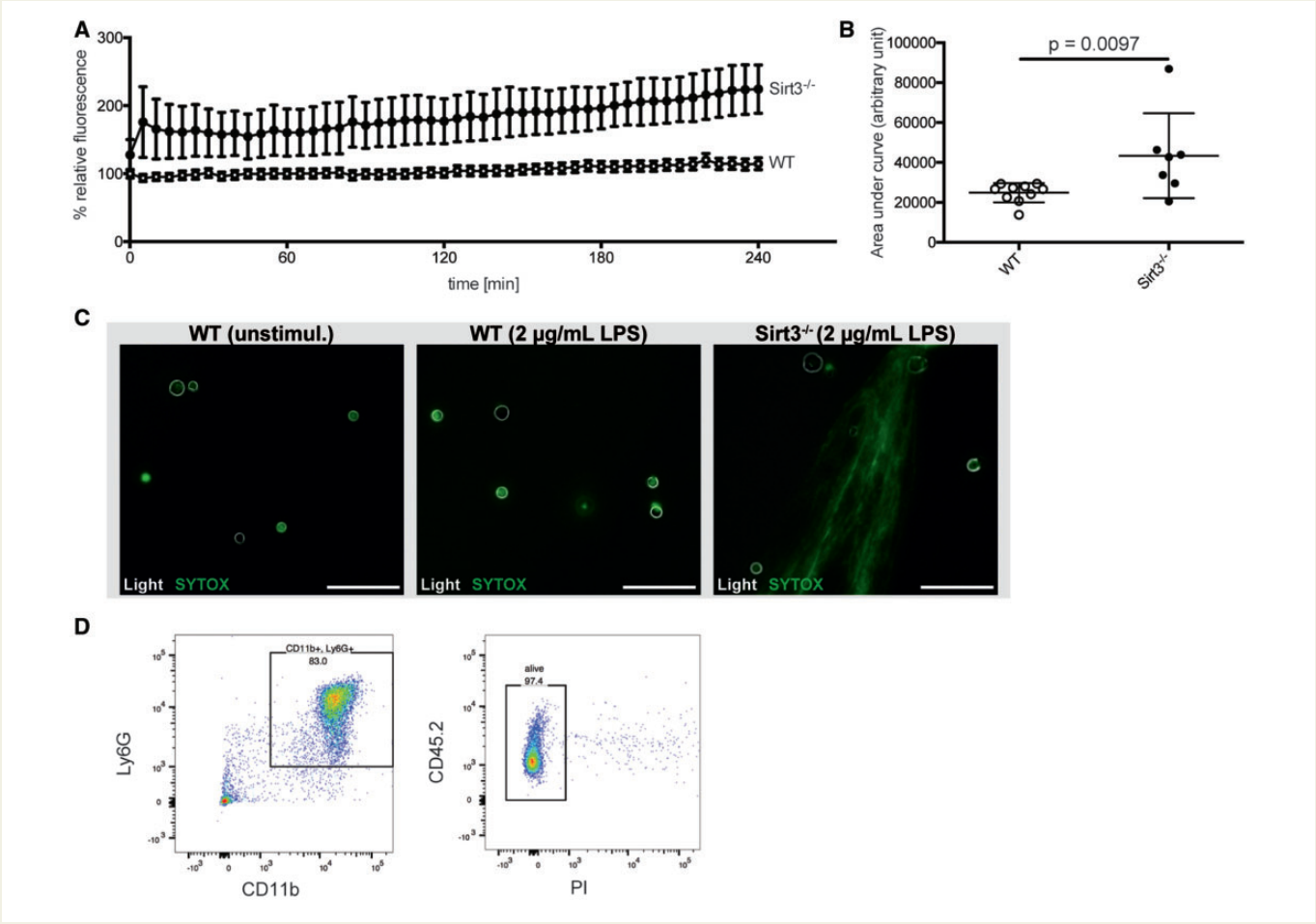

Figure 4 *Sirt3* deficiency favours NET formation in bone marrow-derived mouse neutrophils. NET formation over 4 h was evaluated using SYTOX green nucleic acid stain. *Sirt3*$^{-/-}$ neutrophils (n=10) showed increased NET formation upon stimulation with 2 µg/mL LPS when compared to WT neutrophils (n=7) (*A*). The difference was quantified analysing the area under the curve using the Mann–Whitney test (AUC, *B*). Representative photomicrographs of unstimulated WT as well as stimulated WT and *Sirt3*$^{-/-}$ neutrophils (visualised as white outlines using light microscopy) illustrate NET formation (stained with SYTOX green) in the Sirt3-deficient group after 2-h stimulation with 2 µg/mL LPS (*C*, bar=50 µm). FACS analyses of cells from a WT mouse showed that isolated cells were 83% granulocytes (*D*) and viable (>97%; *E*). Ly6G, Lymphocyte antigen 6 complex locus G6D; CD11b, cluster of differentiation molecule 11b; CD45.2, cluster of differentiation molecule 45 expressed by Ly5.2 bearing mouse strains; PI, phosphatidylinositol.

models of arterial thrombosis supports earlier findings in healthy humans where *SIRT3* was upregulated after intense exercise, to protect against neutrophil-mediated oxidative stress.[25]

The more rapid onset of clotting in our *Sirt3*$^{-/-}$ *ex vivo* model using whole blood could not be reversed after depleting whole blood of its cellular components and platelets. Yet, we found increased amounts of active soluble TF in the plasma as a potential mediator. TF and neutrophils play indeed a major role in arterial thrombosis as both TF plasma levels and neutrophil counts are elevated in ACS patients.[26] Using a mouse model of laser-induced thrombosis, another group showed that TF is expressed by neutrophils and is present in the blood at the site of injury immediately after laser onset. Upon neutrophil depletion, the amount of TF in the blood at the site of injury was decreased.[3] Likewise, TF is associated with and expressed in NETs.[8,24] These findings suggest that TF bound to NETs is the reason for increased amounts of active soluble TF in the plasma.

Taking into account our findings and the detrimental role of NETs in ischemia-reperfusion injury,[27] increased NET formation may explain recent observations in mice, where *Sirt3* deletion impaired left ventricular recovery after myocardial ischaemia.[28]

Lastly, we found decreased transcript levels of *SIRT3* and *SOD2* in CD14^{+} cells of STEMI patients with acute coronary occlusion, while we observed reduced transcription of *Sod2* in neutrophils of *Sirt3*-deficient mice. Previously, a role for *Sirt3* in transcriptional regulation of *Sod2* had only been described in cardiomyocytes via *FoxO3*.[17]

4.1 Limitations

Since loss of *Sirt3* without an additional stressor does not lead to a phenotype, we challenged mice with LPS to mimic a pro-inflammatory state as it occurs in patients with ACS.[29] Even though some triggers of acute arterial thrombosis may have an infectious source such as acute respiratory infections with influenza,[30] CVD may develop as a non-infectious

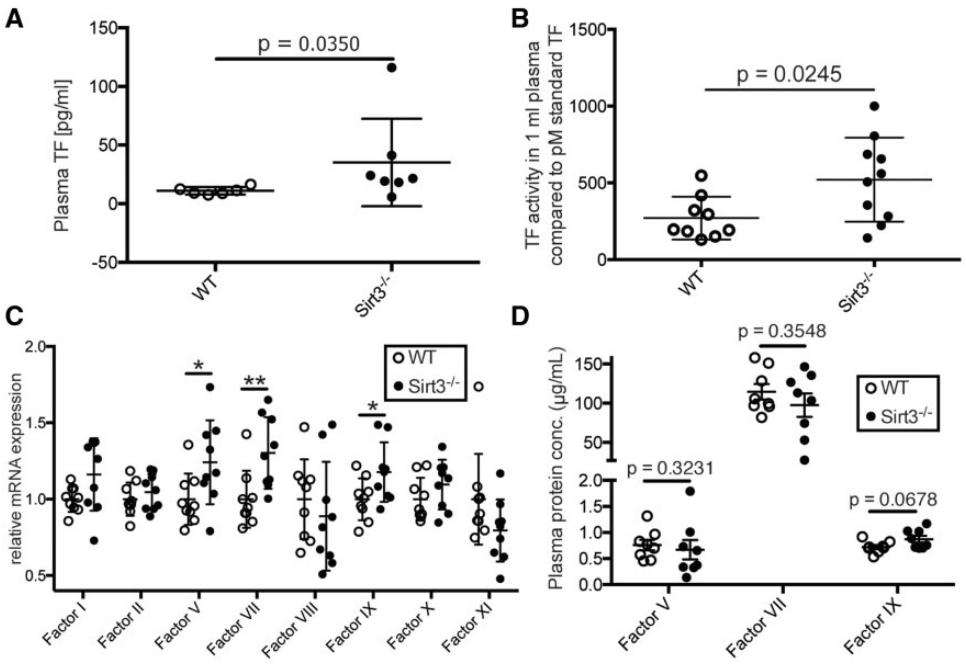

Figure 5 Loss of *Sirt3* increases plasma TF levels and activity. *Sirt3*$^{-/-}$ animals showed increased TF levels (*A*, $n \geq 6$, Mann–Whitney test) and a higher TF activity (*B*, $n \geq 9$, Student's *t*-test) in plasma than in control animals. Liver mRNAs of locally synthesized coagulation factors V, VII, and IX were elevated in *Sirt3*$^{-/-}$ animals (*C*, $n = 9$, *: $P = 0.0385$ and 0.0402; **: $P = 0.0078$, factor VII and XI were analysed using the Mann–Whitney test, the other factors with Student's *t*-test). However, protein plasma levels were not different (*D*, $n = 8$, Factor V analysed by Mann–Whitney test, factors VII and IX by Student's *t*-test).

chronic inflammatory disease.[31] Moreover, recent studies suggest that the gut microbiome enhances CVD and neutrophil pro-inflammatory activity[6,32] and impairs outcome in patients with ACS.[33]

Due to a lack of availability of human neutrophil samples, we used human CD14^{+} leukocytes. With both neutrophils and monocytes being leukocyte subsets, we postulated that a differential expression of *SIRT3* in human monocytes may parallel a differential expression in murine neutrophils. Furthermore, we isolated mouse CD11b^{+} cells, the mouse equivalent to human CD14^{+} cells. Since we could not replicate the changes seen in human CD14^{+} in murine CD11b^{+} cells, our data suggest that an extrapolation between mouse and human leukocytes has to be done with caution. Our findings also suggest that *SOD2* in human neutrophils may not fully account for *SIRT3*-mediated NET formation. A possible reason for the changes in monocytic *SIRT3* expression in humans may lie in the fact that STEMI patients usually suffer from inflammation and atherosclerosis for years before myocardial infarction. Thus, downregulation of *SIRT3* in this case may be a reaction to this chronic condition, which was not replicated in mice apart from exposing them acutely with LPS.

Along the same line, our mouse expertiments highlight a proof-of-principle and *causality* between *Sirt3* deficiency and the thrombosis phenotype in a non-atherosclerotic carotid artery. In humans, context and protagonist cells are different—and we describe an *association* between decreased *SIRT3* in monocytes of STEMI patients. We did not address NETosis and *SIRT3* in humans, yet increased tissue factor and NETosis have been reported in culprit coronary arteries of patients with acute myocardial infarction.[8] Nevertheless, a *Sirt3*-mediated effect on murine NET formation does exist and our data do not exclude an effect of Sirt3-deficiency on human neutrophils. To test the translatability, our findings have to be replicated in neutrophils from human STEMI patients.

Even though increased TF in plasma may be mainly derived from activated neutrophils, monocytes may contribute, as they have been described to release TF microvesicles.[34] It is conceivable that the initial release of TF originates from neutrophils, as they are the first cells to reach the site of injury.[3] Subsequent release of TF from monocytes is likely to be triggered by interactions between neutrophils and the endothelium. Notably, since the discovery of NETs, other types of leukocytes were also shown to release extracellular mitochondrial DNA traps.[35,36] It is possible that these leukocytes contribute to the effects observed *in vivo* and *ex vivo*.

4.2 Conclusions and perspectives

Our study highlights a protective role of *Sirt3* in neutrophils in a mouse model of acute carotid thrombosis under inflammatory conditions. In line with these findings, acute coronary thrombosis in STEMI patients is associated with decreased protective factors such as lower *SIRT3* and *SOD2* levels in CD14^{+} cells. Future studies in neutrophils of patients with myocardial infarction should be done to more specifically address the association between neutrophil-derived SIRT3, SOD2 levels, and NET formation.

Based on our results, we postulate that activation of *SIRT3* in ACS may improve outcome of STEMI patients by reducing NET-dependent procoagulatory properties. As NETs are described in a variety of other non-infectious diseases,[37] *SIRT3* activation may also provide beneficial

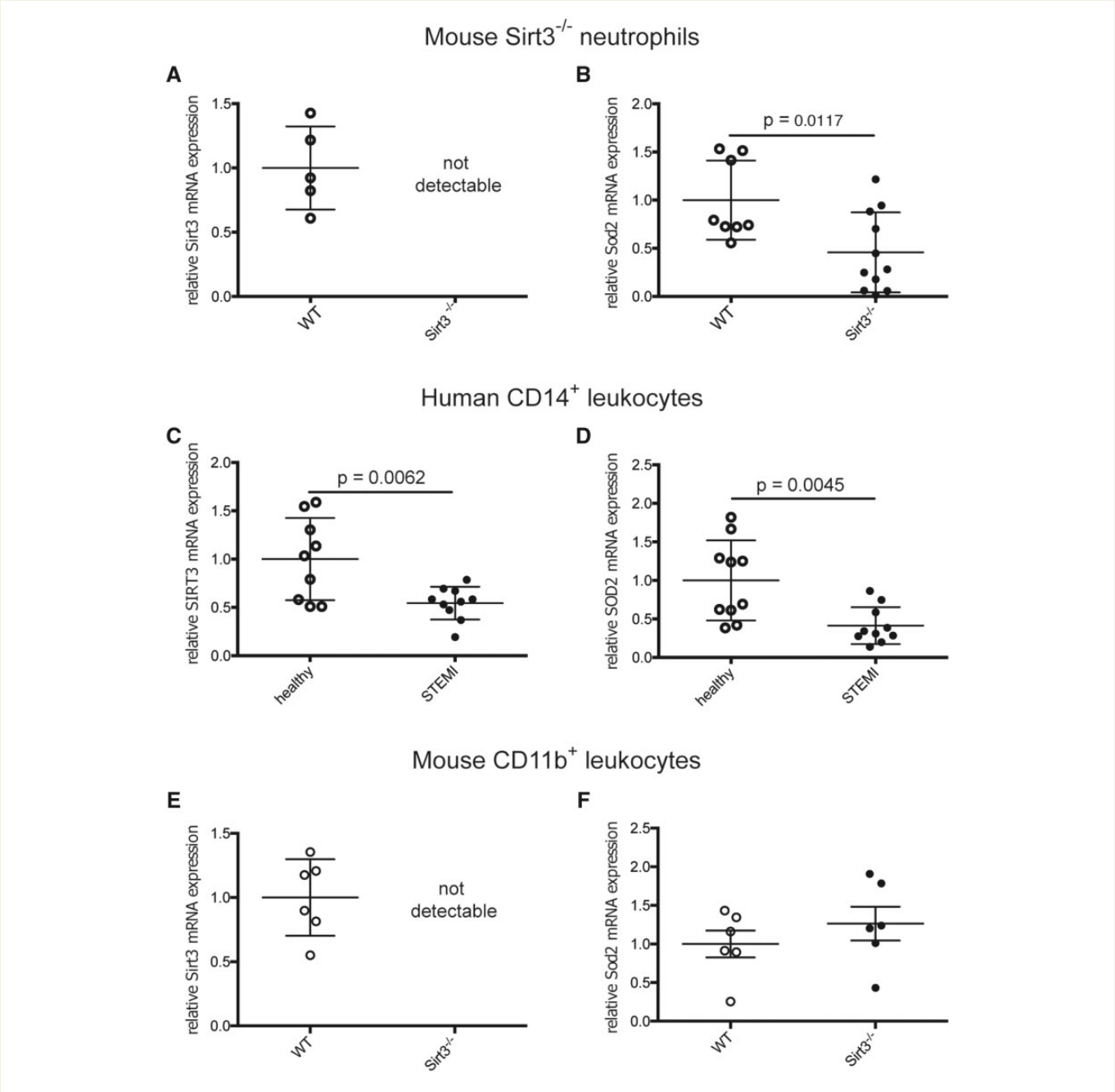

Figure 6 *Sod2* transcription is reduced in *Sirt3*-deficient mouse neutrophils, but not in monocytes—$CD14^+$ leukocytes of STEMI patients show reduced *SIRT3* and *SOD2* transcript levels. Murine *Sirt3*$^{-/-}$ neutrophils lack *Sirt3* (*A*) and show reduced transcription of *Sod2* (*B*, $n \geq 8$, Student's *t*-test). STEMI patients demonstrate reduced mRNA levels of *SIRT3* (*C*) and *SOD2* (*D*) in $CD14^+$ cells compared to healthy donors ($n = 10$, both Student's *t*-test). $CD11b^+$ cells from *Sirt3*-deficient mice show no differential transcription of *Sod2* compared to WT (*E* and *F*, $n = 6$, Mann–Whitney test).

effects in these disease contexts. Indeed, the therapeutic potential of specific sirtuin activators in CVD has been reported.[18] However, to date no clinically effective specific activator of any of the seven sirtuins has been identified. Investing in the discovery of new substances that can specifically activate certain sirtuins could open new therapeutic possibilities for CVD, as well as other metabolic and age-related diseases. Promising alternative approaches could be to boost SIRT3 expression by transcriptional activation or to use CRISPR technology. Finally, since beneficial roles in CVD have been described also for other sirtuins,[18] pan-sirtuin activators appear worthy for clinical testing. Recently, the first pilot study using the NAD^+ precursor nicotinamide riboside (NR) has been completed[38] and on-going clinical studies are investigating the effect of NR on aging, obesity, insulin resistance, and coronary artery disease.

Table 1 Baseline characteristics of healthy donors and STEMI patients

	Healthy	STEMI	*P* value
n	10	10	
Gender (f/m)	4/6	2/8	0.63[a]
Age (years)	58±8	62±9	0.39[b]
BMI (kg/m^2)	24.0±3.1	26.1±3.3	0.13[b]
Time to catheterization (h)	–	6.76±9.3	–
Systolic blood pressure (mmHg)	119.1±9.0	123.2±29.3	0.84[a]
Diastolic blood pressure (mmHg)	71.0±8.8	82.3±16.3	0.046[a]
Diabetes history (f/m)	0/0	0/0	–
Fasting glucose (mmol/L)	5.1±0.6	7.3±1.2	<0.0001[a]
Total cholesterol (mmol/L)	5.3±0.8	5.5±1.6	0.75[b]
HDL (mmol/L)	1.7±0.5	1.3±0.3	0.017[b]
LDL (mmol/L)	3.2±0.6	3.5±1.3	0.47[b]
Triglycerides (mmol/L)	1.0±0.4	0.9±0.4	0.57[b]
CRP (mg/L)	1.3±1.5	11.3±10.5	0.064[a]
Creatinine (μmol/L)	87.3±10.7	83.3±14.3	0.49[b]
Statins (f/m)	0/0	1/3	–
Aspirin (f/m)	0/0	1/2	–

m/f, number of males/females; BMI, body mass index; time to catheterization, time between pain onset and sheath insertion in the catheterization laboratory; HDL, high-density lipoprotein; LDL, low-density lipoprotein; CRP, C-reactive protein. *n* = 10.
[a]Mann–Whitney test.
[b]Student's *t*-test.

Supplementary material

Supplementary material is available at *Cardiovascular Research* online.

Acknowledgements

We thank the catheter team and study nurse Anika Adam at the University Heart Center in Zurich for recruiting patients and healthy donors, and Aliki Buhayer (PRISM Scientific Sàrl) for her support in medical writing. *Figure 7* was designed using Servier Medical Art by Servier under a Creative Commons Attribution 3.0 Unported License.

Conflict of interest: C.M.M. received research grants from Swiss National Science Foundation, from the University Research Priority Program Integrative Human Physiology at the University of Zurich, and from Hartmann-Müller Foundation during the conduct of the study, as well as grants from MSD, Bayer, AstraZeneca, EliLilly, and speaker fees from MSD, AstraZeneca, Roche, Sanofi, and Amgen outside the submitted work. T.F.L. received grants to the institution from Amgen, AstraZeneca, Bayer Healthcare, Biosensors, Biotronik, Boston Scientific, Eli Lilly, Medtronic, MSD, Merck, Roche and Servier, including speaker fees by some of them. S.W. received grants from Biotronik, Bacco Pharmaceutical, Edwards Lifesciences, Medtronic, and Terumo Inc, as well as grants and speaker fees from Boston Scientific and Daiichi Sankyo, all outside the submitted work. J.A. is a founder and scientific advisory board member of Mitobridge.

Funding

This work was supported by the Swiss National Science Foundation [31003 A-140780 to J.A., 310030-135815 to T.F.L., 310030-146923 to

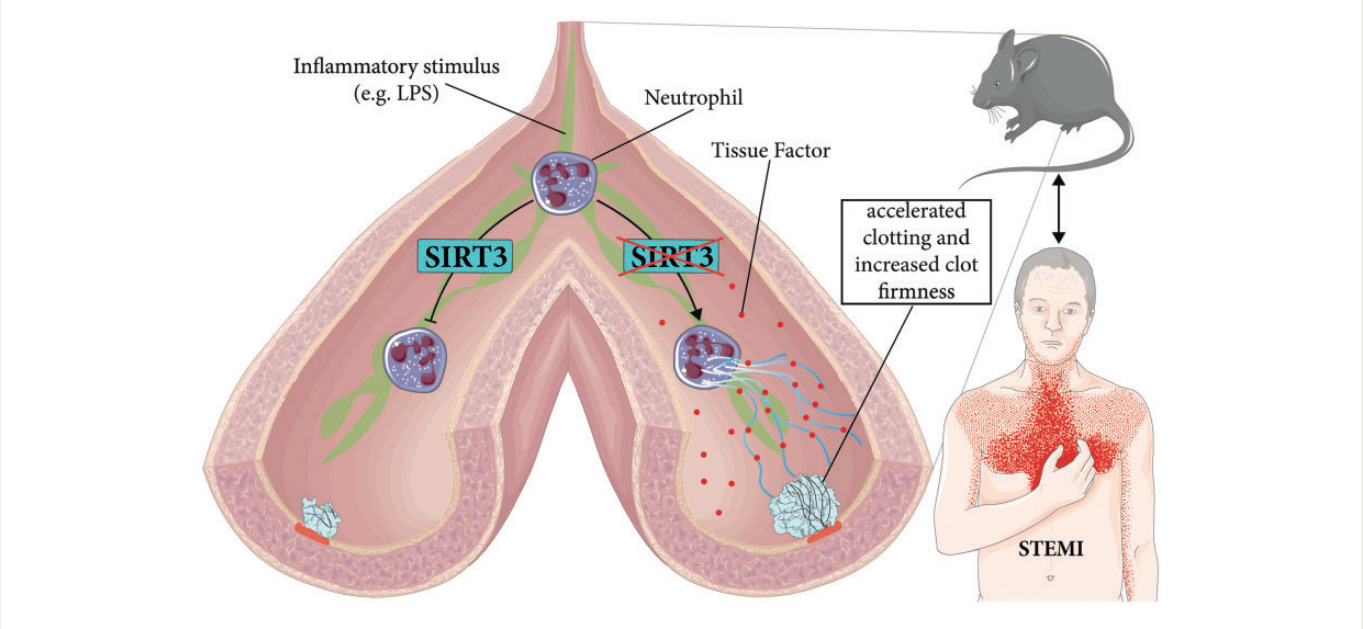

Figure 7 Scheme illustrating prothrombotic effects of *Sirt3* deficiency. Upon pro-inflammatory stimuli such as bacterial endotoxins (e.g. LPS) or oxLDL known to trigger human atherothrombotic events, endogenous *Sirt3* protects neutrophils from NET formation (left). In contrast, absence of *Sirt3* favours NETs, thereby accelerating clotting and increasing clot firmness (right) in mice. In patients with STEMI, *SIRT3* transcription levels are reduced.

C.M.M., 310030-165990 to C.M.M. and J.A., 32473B-163271 to F.M., 33CM30-140336 to SPUM-ACS]; the National Institute of Health (USA) [R01AG043930 to J.A.]; the University Research Priority Program Integrative Human Physiology at the University of Zurich to [C.M.M. and D.S.G.]; the Hartmann-Müller Foundation to [C.M.M. and L.J.v.T.]; the Ecole Polytechnique Fédérale de Lausanne to [J.A.]; the University of Zurich to [C.M.M. and S.W.]; the Swiss Heart Foundation (to C.M.M); and the Foundation for Cardiovascular Research, Zurich, Switzerland.

References

1. Townsend N, Wilson L, Bhatnagar P, Wickramasinghe K, Rayner M, Nichols M. Cardiovascular disease in Europe: epidemiological update 2016. *Eur Heart J* 2016;**37**:3232–3245.
2. Görlach A. Redox regulation of the coagulation cascade. *Antioxid Redox Signal* 2005;**7**:1398–1404.
3. Darbousset R, Thomas GM, Mezouar S, Frère C, Bonier R, Mackman N, Renné T, Dignat-George F, Dubois C, Panicot-Dubois L. Tissue factor-positive neutrophils bind to injured endothelial wall and initiate thrombus formation. *Blood* 2012;**120**:2133–2143.
4. Lood C, Blanco LP, Purmalek MM, Carmona-Rivera C, De Ravin SS, Smith CK, Malech HL, Ledbetter JA, Elkon KB, Kaplan MJ. Neutrophil extracellular traps enriched in oxidized mitochondrial DNA are interferogenic and contribute to lupus-like disease. *Nat Med* 2016;**22**:146–153.
5. Brinkmann V, Reichard U, Goosmann C, Fauler B, Uhlemann Y, Weiss DS, Weinrauch Y, Zychlinsky A. Neutrophil extracellular traps kill bacteria. *Science* 2004;**303**:1532–1535.
6. Kelly TN, Bazzano LA, Ajami NJ, He H, Zhao J, Petrosino JF, Correa A, He J. Gut microbiome associates with lifetime cardiovascular disease risk profile among bogalusa heart study participants. *Circ Res* 2016;**119**:956–964.
7. Fuchs TA, Abed U, Goosmann C, Hurwitz R, Schulze I, Wahn V, Weinrauch Y, Brinkmann V, Zychlinsky A. Novel cell death program leads to neutrophil extracellular traps. *J Cell Biol* 2007;**176**:231–241.
8. Stakos DA, Kambas K, Konstantinidis T, Mitroulis I, Apostolidou E, Arelaki S, Tsironidou V, Giatromanolaki A, Skendros P, Konstantinides S, Ritis K. Expression of functional tissue factor by neutrophil extracellular traps in culprit artery of acute myocardial infarction. *Eur Heart J* 2015;**36**:1405–1414.
9. Massberg S, Grahl L, von Bruehl ML, Manukyan D, Pfeiler S, Goosmann C, Brinkmann V, Lorenz M, Bidzhekov K, Khandagale AB, Konrad I, Kennerknecht E, Reges K, Holdenrieder S, Braun S, Reinhardt C, Spannagl M, Preissner KT, Engelmann B. Reciprocal coupling of coagulation and innate immunity via neutrophil serine proteases. *Nat Med* 2010;**16**:887–896.
10. Mangold A, Alias S, Scherz T, Hofbauer T, Jakowitsch J, Panzenbock A, Simon D, Laimer D, Bangert C, Kammerlander A, Mascherbauer J, Winter MP, Distelmaier K, Adlbrecht C, Preissner KT, Lang IM. Coronary neutrophil extracellular trap burden and deoxyribonuclease activity in ST-elevation acute coronary syndrome are predictors of ST-segment resolution and infarct size. *Circ Res* 2015;**116**:1182–1192.
11. Guarente L, Franklin H, Epstein L. Sirtuins, aging, and medicine. *N Engl J Med* 2011;**364**:2235–2244.
12. Houtkooper RH, Pirinen E, Auwerx J. Sirtuins as regulators of metabolism and healthspan. *Nat Rev Mol Cell Biol* 2012;**13**:225–238.
13. Breitenstein A, Stein S, Holy EW, Camici GG, Lohmann C, Akhmedov A, Spescha R, Elliott PJ, Westphal CH, Matter CM, Luscher TF, Tanner FC. Sirt1 inhibition promotes in vivo arterial thrombosis and tissue factor expression in stimulated cells. *Cardiovasc Res* 2011;**89**:464–472.
14. Kumari S, Chaurasia SN, Nayak MK, Mallick RL, Dash D. Sirtuin inhibition induces apoptosis-like changes in platelets and thrombocytopenia. *J Biol Chem* 2015;**290**:12290–12299.
15. Bell EL, Guarente L. The SirT3 divining rod points to oxidative stress. *Mol Cell* 2011;**42**:561–568.
16. Qiu X, Brown K, Hirschey MD, Verdin E, Chen D. Calorie restriction reduces oxidative stress by SIRT3-mediated SOD2 activation. *Cell Metab* 2010;**12**:662–667.
17. Sundaresan NR, Gupta M, Kim G, Rajamohan SB, Isbatan A, Gupta MP. Sirt3 blocks the cardiac hypertrophic response by augmenting Foxo3a-dependent antioxidant defense mechanisms in mice. *J Clin Invest* 2009;**119**:2758–2771.
18. Winnik S, Auwerx J, Sinclair DA, Matter CM. Protective effects of sirtuins in cardiovascular diseases: from bench to bedside. *Eur Heart J* 2015;**36**:3404–3412.
19. Lombard DB, Alt FW, Cheng HL, Bunkenborg J, Streeper RS, Mostoslavsky R, Kim J, Yancopoulos G, Valenzuela D, Murphy A, Yang Y, Chen Y, Hirschey MD, Bronson RT, Haigis M, Guarente LP, Farese RV, Weissman S, Verdin E, Schwer B. Mammalian Sir2 homolog SIRT3 regulates global mitochondrial lysine acetylation. *Mol Cell Biol* 2007;**27**:8807–8814.
20. Winnik S, Gaul DS, Siciliani G, Lohmann C, Pasterk L, Calatayud N, Weber J, Eriksson U, Auwerx J, van Tits LJ, Lüscher TF, Matter CM. Mild endothelial dysfunction in Sirt3 knockout mice fed a high-cholesterol diet: protective role of a novel C/EBP-β-dependent feedback regulation of SOD2. *Basic Res Cardiol* 2016;**111**:33.
21. Winnik S, Gaul DS, Preitner F, Lohmann C, Weber J, Miranda MX, Liu Y, Tits LJ, Mateos JM, Brokopp CE, Auwerx J, Thorens B, Lüscher TF, Matter CM. Deletion of Sirt3 does not affect atherosclerosis but accelerates weight gain and impairs rapid metabolic adaptation in LDL receptor knockout mice: implications for cardiovascular risk factor development. *Basic Res Cardiol* 2014;**109**:399.
22. Fernandez-Marcos PJ, Jeninga EH, Canto C, Harach T, de Boer VC, Andreux P, Moullan N, Pirinen E, Yamamoto H, Houten SM, Schoonjans K, Auwerx J. Muscle or liver-specific Sirt3 deficiency induces hyperacetylation of mitochondrial proteins without affecting global metabolic homeostasis. *Sci Rep* 2012;**2**:425.
23. Swamydas M, Luo Y, Dorf ME, Lionakis MS. Isolation of mouse neutrophils. *Curr Protoc Immunol* 2015;**110**:3.20.21–23.20.15.
24. Kambas K, Chrysanthopoulou A, Vassilopoulos D, Apostolidou E, Skendros P, Girod A, Arelaki S, Froudarakis M, Nakopoulou L, Giatromanolaki A, Sidiropoulos P, Koffa M, Boumpas DT, Ritis K, Mitroulis I. Tissue factor expression in neutrophil extracellular traps and neutrophil derived microparticles in antineutrophil cytoplasmic antibody associated vasculitis may promote thromboinflammation and the thrombophilic state associated with the disease. *Ann Rheum Dis* 2014;**73**:1854–1863.
25. Ferrer MD, Tauler P, Sureda A, Tur JA, Pons A. Antioxidant regulatory mechanisms in neutrophils and lymphocytes after intense exercise. *J Sports Sci* 2009;**27**:49–58.
26. Seljeflot I, Hurlen M, Hole T, Arnesen H. Soluble tissue factor as predictor of future events in patients with acute myocardial infarction. *Thromb Res* 2003;**111**:369–372.
27. Ge L, Zhou X, Ji WJ, Lu RY, Zhang Y, Zhang YD, Ma YQ, Zhao JH, Li YM. Neutrophil extracellular traps in ischemia-reperfusion injury-induced myocardial no-reflow: therapeutic potential of DNase-based reperfusion strategy. *Am J Physiol Heart Circ Physiol* 2015;**308**:H500–H509.
28. He X, Zeng H, Chen JX. Ablation of SIRT3 causes coronary microvascular dysfunction and impairs cardiac recovery post myocardial ischemia. *Int J Cardiol* 2016;**215**:349–357.
29. Maier W, Altwegg LA, Corti R, Gay S, Hersberger M, Maly FE, Sütsch G, Roffi M, Neidhart M, Eberli FR, Tanner FC, Gobbi S, von Eckardstein A, Lüscher TF. Inflammatory markers at the site of ruptured plaque in acute myocardial infarction: locally increased interleukin-6 and serum amyloid A but decreased C-reactive protein. *Circulation* 2005;**111**:1355–1361.
30. Kwong JC, Schwartz KL, Campitelli MA, Chung H, Crowcroft NS, Karnauchow T, Katz K, Ko DT, McGeer AJ, McNally D, Richardson DC, Rosella LC, Simor A, Smieja M, Zahariadis G, Gubbay JB. Acute myocardial infarction after laboratory-confirmed influenza infection. *N Engl J Med* 2018;**378**:345–353.
31. Ridker PM, Everett BM, Thuren T, MacFadyen JG, Chang WH, Ballantyne C, Fonseca F, Nicolau J, Koenig W, Anker SD, Kastelein JJP, Cornel JH, Pais P, Pella D, Genest J, Cifkova R, Lorenzatti A, Forster T, Kobalava Z, Vida-Simiti L, Flather M, Shimokawa H, Ogawa H, Dellborg M, Rossi PRF, Troquay RPT, Libby P, Glynn RJ, Group CT. Antiinflammatory therapy with canakinumab for atherosclerotic disease. *N Engl J Med* 2017;**377**:1119–1131.
32. Zhang D, Chen G, Manwani D, Mortha A, Xu C, Faith JJ, Burk RD, Kunisaki Y, Jang JE, Scheiermann C, Merad M, Frenette PS. Neutrophil ageing is regulated by the microbiome. *Nature* 2015;**525**:528–532.
33. Li XS, Obeid S, Klingenberg R, Gencer B, Mach F, Raber L, Windecker S, Rodondi N, Nanchen D, Muller O, Miranda MX, Matter CM, Wu Y, Li L, Wang Z, Alamri HS, Gogonea V, Chung YM, Tang WH, Hazen SL, Luscher TF. Gut microbiota-dependent trimethylamine N-oxide in acute coronary syndromes: a prognostic marker for incident cardiovascular events beyond traditional risk factors. *Eur Heart J* 2017;**38**:814–824.
34. Falati S, Liu Q, Gross P, Merrill-Skoloff G, Chou J, Vandendries E, Celi A, Croce K, Furie BC, Furie B. Accumulation of tissue factor into developing thrombi in vivo is dependent upon microparticle P-selectin glycoprotein ligand 1 and platelet P-selectin. *J Exp Med* 2003;**197**:1585–1598.
35. Yousefi S, Gold JA, Andina N, Lee JJ, Kelly AM, Kozlowski E, Schmid I, Straumann A, Reichenbach J, Gleich GJ, Simon HU. Catapult-like release of mitochondrial DNA by eosinophils contributes to antibacterial defense. *Nat Med* 2008;**14**:949–953.
36. Morshed M, Hlushchuk R, Simon D, Walls AF, Obata-Ninomiya K, Karasuyama H, Djonov V, Eggel A, Kaufmann T, Simon HU, Yousefi S. NADPH oxidase-independent formation of extracellular DNA traps by basophils. *J Immunol* 2014;**192**:5314–5323.
37. Jorch SK, Kubes P. An emerging role for neutrophil extracellular traps in noninfectious disease. *Nat Med* 2017;**23**:279–287.
38. Trammell SA, Schmidt MS, Weidemann BJ, Redpath P, Jaksch F, Dellinger RW, Li Z, Abel ED, Migaud ME, Brenner C. Nicotinamide riboside is uniquely and orally bioavailable in mice and humans. *Nat Comms* 2016;**7**:12948.